STRONG GROUND MOTION CHARACTERISTICS DURING SIGNIFICANT EARTHQUAKES AT BMKG ACCELEROGRAPH STATIONS: JGPI AND JBPI

A.P Budi [1] , Jambari [1] , D. Pamuji [1]
[1]Stasiun Geofisika Kelas I Jayapura, 99114, [2]BBMKG Wilayah V Jayapura , 99114
email: achmad.budi@bmkg.go.id

Recieved: April 29, 2022 Reviewed: August 11, 2022 Accepted: October 13, 2025

ABSTRACT

Jayapura City is an area with high seismicity, dense population, and rapid development, making it more vulnerable to earthquake damage. This study analyzed ground motion characteristics, which include peak ground acceleration (PGA), effective duration, and response spectral acceleration, using data on four earthquakes that hit the city in 2021-2022. PGA value is determined by identifying the peak of the spectrum, whereas the total response acceleration is obtained and plotted in a graph of the period against the amplitude. Meanwhile, the effective duration is based on the concept of significant duration, with the interval of Arias intensity of 5–95%. Ground motion acceleration data were obtained from the Meteorological, Climatological, and Geophysical Agency (Badan Meteorologi, Klimatologi, dan Geofisika/BMKG) accelerograph stations, namely JGPI and JBPI Stations. The analysis results reveal a higher PGA value in JGPI Station than in JBPI Station. This is due to the site conditions of JGPI Station as hard soil. In addition to resonating at high frequencies, hard soil also has a high damping effect which results in shorter effective duration. Conversely, the effective duration is longer in the JBPI Station than in the JGPI Station due to its relatively softer soil conditions. Furthermore, the response spectral acceleration values of all earthquakes recorded at both JBPI and JGPI Stations are lower than those of response spectra designs in SNI 1726:2019. This indicates that the earthquakes were felt but did not cause significant damage, as per the actual condition.

Keywords: PGA, effective duration, response spectrum

1. Introduction

Papua Island has complex geological conditions due to the interactions of the Indo-Australian and Carolina tectonic plates [1-3]. These interactions produce several major deformation zones on this island, which include the Sorong Fault Zone, Yapen Fault Zone, Mamberamo Fault Zone, Manokwari Trough, and New Guinea Trench. The Mamberamo Fault Zone, which stretches from Jayapura to the eastern tip of Yapen Island, is one of the active intraplate faults on Papua Island. This fault is horizontal and has a West-East orientation. Furthermore, Bukit Nawa located to the south of Jayapura consists mainly of Mesozoic rock hills and mud deposits from poton/mud volcano eruptions [4-5]. Thrust faults with a northwest-southeast orientation border the hills and mudflats. The Waruta, Pawasi, and Anabranch faults are the three primary faults in this area, and the majority of the earthquakes that occur have a thrust fault mechanism.

As the provincial capital, Jayapura City has become the hub of urbanization in Papua, resulting in increased population growth over the years. In 2022, the population of Jayapura City reached 300,192 people [6]. Such a dense population poses a high risk of earthquakes in this city. Building quality that does not comply with SNI standards, buildings that are situated on soft soil, and the energy produced by the earthquake all contribute to the amount of damage caused by seismic shocks. To determine the strength demand in the form of horizontal force due to an earthquake, a spectrum response from the earthquake is required [7]. On Papua Island, significant earthquakes happen along strike-slip faults such as the Sorong Fault and the Mamberamo Fault Zone, as well as subduction along the Papua New Guinea Trench. Shallow earthquakes with Mw > 6 mostly have a strike-slip mechanism and occur around the Sorong Fault and the Mamberamo Fault Zone. Data from past earthquakes indicates that several devastating earthquakes have shaken the Papua region, including the Sarmi Earthquake on 20

June 2019 (M6.3), which caused significant damage to 33 houses, and the Papua New Guinea Earthquake on 17 Juli 1998 (M8.7), which triggered a tsunami in the region of Jayapura [8].

Hiola et al. conducted a study on the determination of PGA value and effective duration of the 2018 Lebak Earthquake and reported that the closer the accelerograph station is to the earthquake epicenter, the greater the PGA value [9]. Conversely, the further the distance of the station to the epicenter, the longer the effective duration. According to Herrmann et al. who identified the significant directivity effects of the L'Aquila Earthquake (Mw 6.3) on 6 April 2009, stations oriented along the fault direction tend to have high amplitude and short ground motion duration, and vice versa [10]. Mahani et al. analyzed the strong ground motion of the Kermanshah Earthquake which occurred on 12 November 2017 in western Iran (M7.3) and revealed that the amplitude of the earthquake is dominated by long-period pulses. Although the PGA of the M7.3 Kermanshah Earthquake seems to be higher than the global value for the NEHRP class B site, a comparison of the peak ground acceleration in the horizontal component (PGA) of the M7.3 earthquake with the global PGA values reveals a similar decrease in ground motion amplitude [11].

This study aims to determine the PGA value, effective duration, and comparison of spectral acceleration on significant earthquakes in Jayapura with Response Spectra Designs in SNI 1726-2019.

PGA is the largest absolute acceleration amplitude recorded on an accelerogram at a seismic station during a particular earthquake. It is also known as an intensity measure to describe the level of earthquake shaking [12]. The effective duration of an earthquake (Td) is the duration of the accumulation of squared integral values, which is limited to 5–95% of the total earthquake recordings [13]. Earthquake recordings are generally divided into 3 parts. The first part is the initial weak part, the second part is the strong part that contributes most of the energy or causes damage and is considered the effective duration of the earthquake, and the third part is the final weak part. Response Spectra Design is a curve of the acceleration function against the period that refers to the 2017 Indonesian Earthquake Source and Hazard Map and SNI 1726:2019 to determine the earthquake load at a location.

Based on their geological conditions (Figure 1), both JGPI and JBPI accelerograph stations are situated above ultramafic rocks, which are composed of harzburgite and serpentinite minerals, in the Cycloop Mountains area [14]. Meanwhile, according to their topographic conditions, JGPI Station is located on the slope of the Cycloop Mountains at an elevation of 444.9 m, whereas JBPI Station is situated near the north coast of Papua Island at the base of the Cycloop Mountains at a height of 41 m.

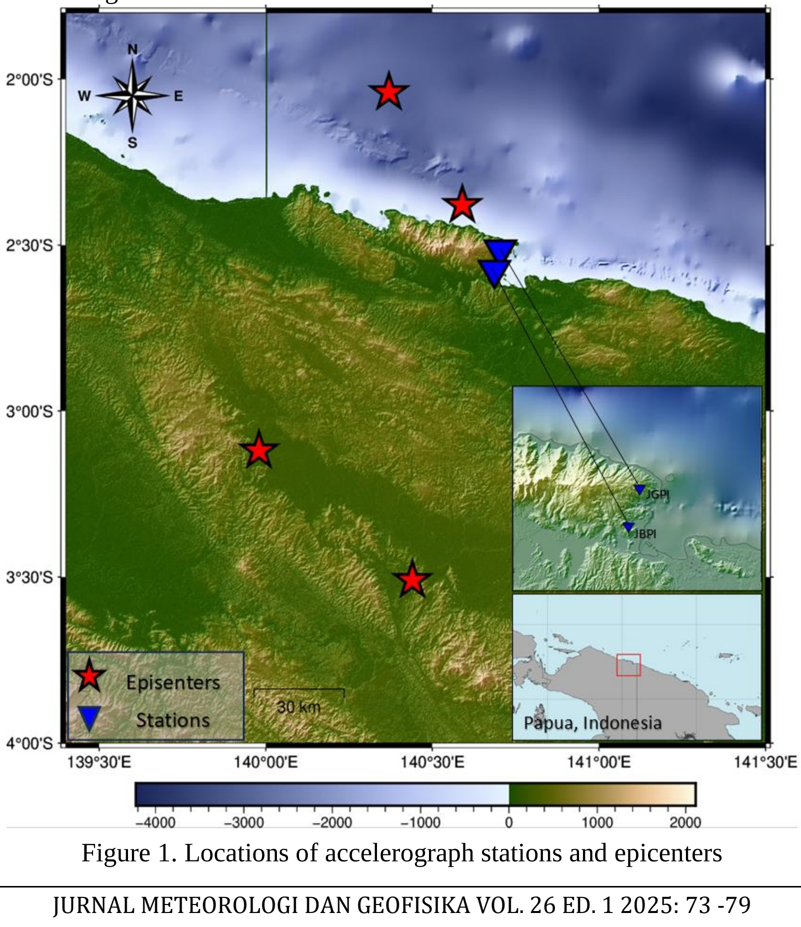

Figure 1. Locations of accelerograph stations and epicenters

2. Methods

Data collection. Earthquake ground acceleration recording data were obtained from the BMKG accelerograph station (JGPI) located at Jayapura Geophysical Station and the seismic station (JBPI) located at the Center for Meteorology, Climatology, and Geophysics Agency Region V Jayapura (*Balai Besar Meteorologi Klimatologi dan Geofisika* (BBMKG) *Wilayah 5 Jayapura*). The data include those of the Keerom earthquake (M5.7) on 28 August 2021, the North Jayapura earthquake (M5.5) on 20 January 2022, the North Jayapura earthquake (M4.0) on 29 March 2022, and the Jayapura Regency earthquake (M5.2) on 9 April 2022.

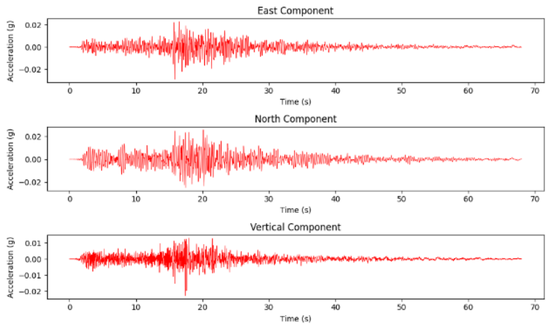

Figure 2. Ground motion acceleration recordings of Keerom earthquake, 28 August 2021 (M5.7), at JGPI Station

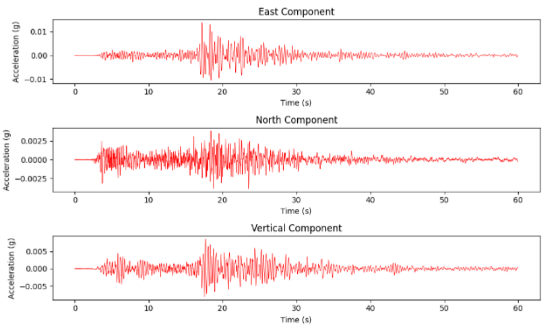

Figure 3. Ground motion acceleration recordings of Keerom earthquake, 28 August 2021 (M5.7), at JBPI Station

Ground motion acceleration data taken from the accelerograph stations consist of three components, namely North-South (NS), East-West (EW), and Vertical (Z). From the three components, the one with the maximum deviation was selected for analysis in determining the PGA value (Figures 2-3).

Data processing. Maximum ground acceleration values of the three components (NS, EW, and Z) were processed to obtain the earthquakes' PGA values, response spectra, and effective durations.

Response spectrum is a graph that illustrates the load response of an earthquake for a certain damping ratio to the period of the vibrating structure [7]. Factors that affect the response spectrum value are earthquake load, vibration period of the structure (T), damping ratio (ξ), ductility level (μ), and site conditions at the accelerograph station. Response spectral acceleration is the most frequently used type of spectrum to determine earthquake loads. This follows Newton's Second Law of Motion that a force is the product of mass and acceleration.

$$F = m.a \quad (1)$$

The generation of a structural reaction requires a Single Degree of Freedom (SDOF) structural model, where the elastic response of a structure that experiences an earthquake in all dimensions is represented as a single mass moving in a single direction, i.e., horizontally [7]. According to Duhamel's principle [19], the differential equation for the motion of an SDOF structure with an earthquake load having an acceleration of y_t is:

$$y(t) = \frac{1}{m\omega_d}\int_0^t \ddot{y}_t e^{-\omega t} \sin \square_d (t-\tau)d\tau \quad (2)$$

where y(t) is mass deviation, ω_d is damping frequency, and m is mass. Thus, mass deviation varies as a function of time. After determining the mass deviation, the mass velocity and acceleration can be calculated using the following equations:

$$\dot{y} = \omega\, y \quad (3)$$

$$\ddot{y} = \omega y \quad (4)$$

However, these equations are merely approximations since the velocity and acceleration history does not occur in the same phase as the displacement history. Therefore, the relationship is analogous to the following equations:

$$PSV\ T = \omega SD(,T) \quad (5)$$

$$PSA\ T = \omega^2 SD(,T) \quad (6)$$

with PSV and PSA being pseudo spectral velocity dan pseudo spectral acceleration, respectively. According to Uang and Bertaro (1990), for a structure with a vibration period of 0.20 < T < 5.0 seconds, the PSV and PSA values are extremely close to the exact values of spectral velocity and spectral acceleration. [15].

The obtained strong motion data were processed using SeismoSignal software [16]. Meanwhile, the response spectral acceleration of an earthquake was processed by inputting data on the sampling time range and acceleration values at the accelerograph station. After that, the data was processed to produce a response spectrum graph (earthquake acceleration against period) with a damping factor of 5%.

To calculate the effective duration, the sampling rate data was multiplied by the square of the acceleration, and the data was accumulated. After that, the accumulated result values were normalized in percentage and plotted in a graph for easier analysis. The relationship between the duration during the earthquake and the percentage of accumulated integral acceleration was plotted in a table, with the minimum percentage of 5% being T1 and the maximum percentage of 95% being T2. Therefore;

$$T_d = T_2 - T_1 \qquad (7)$$

The duration of strong ground motion is one of the main parameters to describe the impact of the shaking caused by an earthquake. Theoretically, earthquakes that have a long duration will cause greater damage. However, this is not always the case as numerous other factors may influence the destructive power of an earthquake. In general, the duration of earthquake vibrations is measured from the moment the signal begins until it stops, which is often referred to as the total duration (Tt). In reality, however, the assessment of total duration is not accurate to indicate potential damage. Thus, the second part of the earthquake recording—the strong part of the earthquake recording or the effective duration—must be understood to determine how long this part affects the potential damage. [7]

3. Results and Discussion

The largest PGA value (0.55 g) was recorded in JGPI Station on the earthquake that occurred on 29 March 2022 (M4.0), while the smallest PGA value was recorded in JBPI Station on the occurrence of an earthquake on 20 January 2022 (M5.5). The PGA values of all earthquakes are shown in Table 1.

As shown in Table 1, the PGA value at the JGPI station is proportional to the PGA value produced, where the closer the distance to the epicenter, the greater the PGA value produced. However, this does not apply to the JBPI station, where there is no direct proportionality between the PGA value and the distance to the epicenter, indicating other factors that influence the PGA value. The following are the comparison graphs of PGA values between JGPI and JBPI stations.

Table 1. PGA value calculation results

Occurrence Date	Epicenter	Magnitude	Depth (km)	JGPI (g)	Distance (Km)	JBPI (g)	Distance (Km)
28-Aug-21	140.44E;3.51S	5.7	48	0.093	115	0.062	108
20-Jan-22	140.37E;2.04S	5.5	10	0.42	64	0.047	68
29-Mar-22	140.59E;2.38S	4.0	10	0.55	19	0.056	23
9-Apr-22	139.98E;3.12S	5.2	53	0.2	110	0.063	104

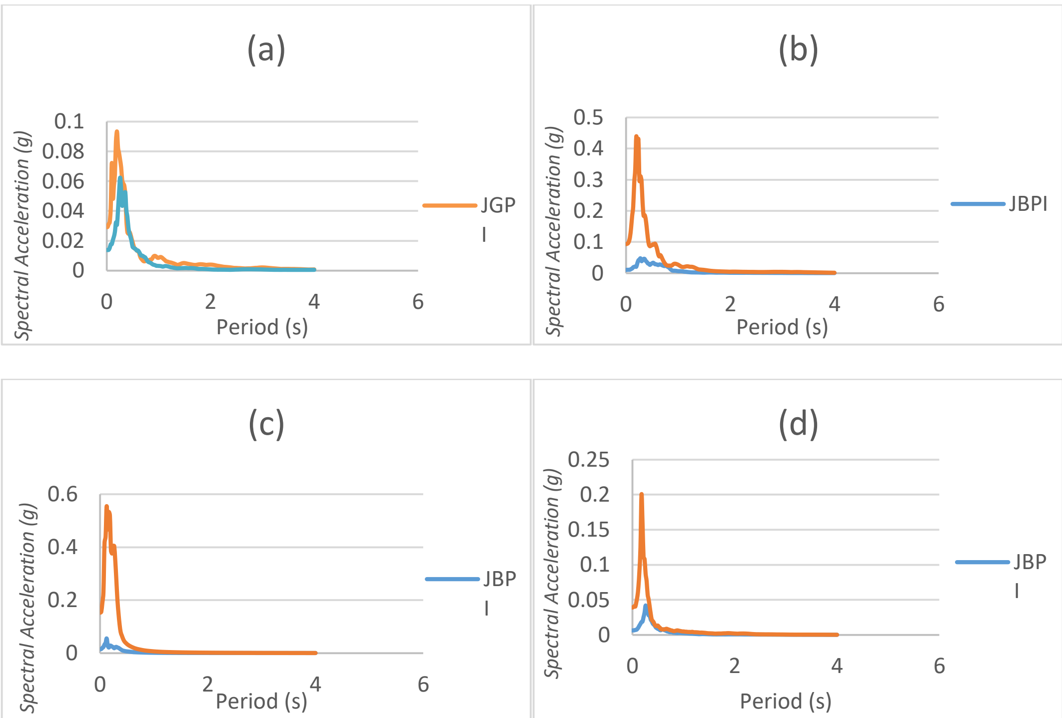

Figure 4. Comparison of response spectral accelerations at JBPI and JGPI Stations: (a) 28 August 2021 (M5.7); (b) 20 January 2022 (M5.5); (c) 29 March 2022 (M4); and (d) 9 April 2022 (M5.2)

As seen in Figure 4 (a, b, c, and d), the PGA values recorded at JGPI Station are greater than those recorded at JBPI Station. According to the topography and geology, the soil at JGPI Station is comparatively harder than that at JBPI Station [14]. This is consistent with how PGA functions in hard and soft soils [17]. JGPI Station, which is relatively farther away from the epicenter of the earthquake, produces a high PGA value. In this condition, the high frequency generated by the earthquake waves causes the hard soil to vibrate, which results in a relatively large material damping at a high PGA because the soil reaction may become inelastic. Thus, the possibility of amplified earthquake waves is relatively small. In addition to distance and magnitude factors, site conditions also affect the magnitude of PGA caused by an earthquake.

The results of the calculation of the effective duration of the four significant earthquakes show that JBPI Station has a longer duration than JGPI Station. Site conditions, earthquake distance, magnitude, and other factors can affect the effective duration values at each station. The effective duration values of all earthquakes at each station are presented in Table 2.

Table 2. Effective duration calculation results

Earthquake	JGPI (dt)	JBPI (dt)
28-Aug-21 (M5.7)	28.45	32.47
20-Jan-22 (M5.5)	17.98	21.83
29-Mar-22 (M4.0)	5.33	9.26
9-Apr-22 (M5.2)	24.7	27.87

The relatively longer effective duration at JBPI Station is due to the site conditions at this station. According to the geological and topographic conditions, JBPI Station has relatively softer soil and lower elevation than JGPI Station. Therefore, the low-frequency content of an earthquake will be associated with soft soil. Consequently, relatively small material damping on soft soil will result in relatively larger amplification. Figure 5 displays the effective duration graphs.

The longest effective duration (32.27 s) was recorded in the occurrence of an earthquake on 28 August 2021 (M5.7) at JBPI Station. This is because JBPI Station has relatively softer soil, allowing low-frequency content to associate with the site conditions at this station. Similarly, the effective duration of all other earthquakes at JBPI Station is always longer than that at JGPI Station. As shown in Table 2, in the earthquakes that occurred on 20 January 2022 (M5.5) and 29 March 2022 (M4.0), the effective duration is relatively longer at JBPI Station (Table 2). This is because the distance between the station and the epicenter affects the duration of the shaking since the propagation of the waves requires a long time to reach the minimum limit of the effective duration of the earthquake, namely 5% [13]. The comparisons of response spectral accelerations of significant earthquakes with response spectra designs in SNI 1726:2019 [18] at both stations for the classification of hard soil (SC), medium soil (SD), and soft soil (SE) are presented in Figures 6 and 7

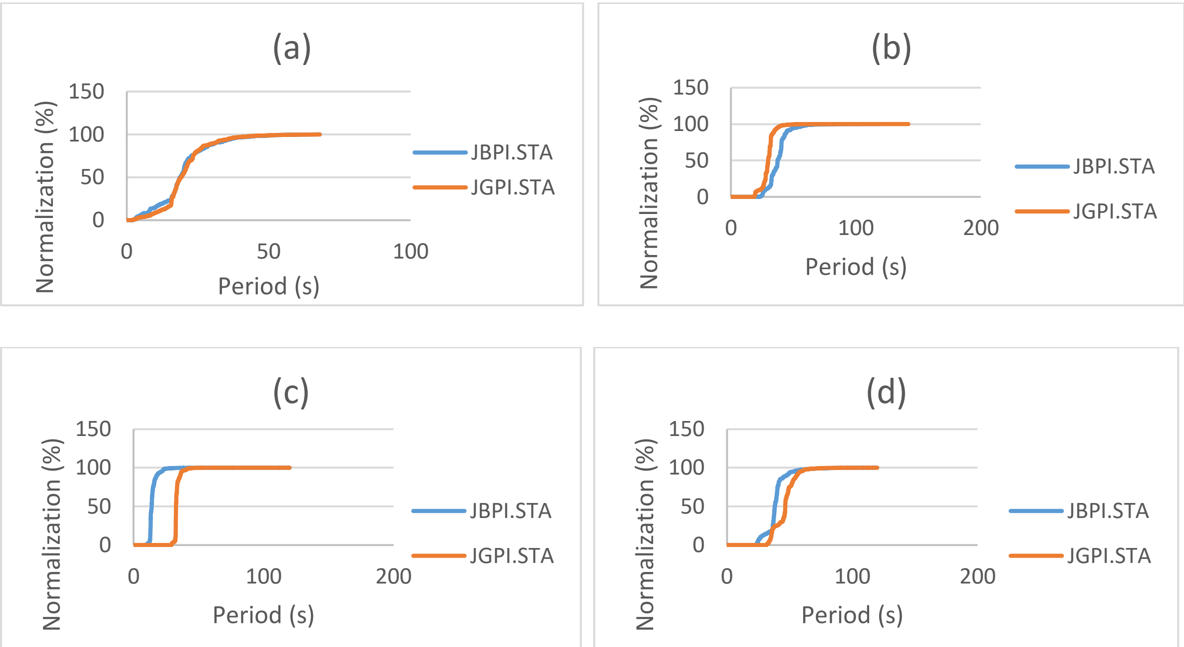

Figure 5. Comparison of effective duration recorded at JGPI and JBPI stations: (a) 28 August 2021 (M5.7); (b) 20 January 2022 (M5.5); (c) 29 March 2022 (M4); and (d) 9 April 2022 (M5.2)

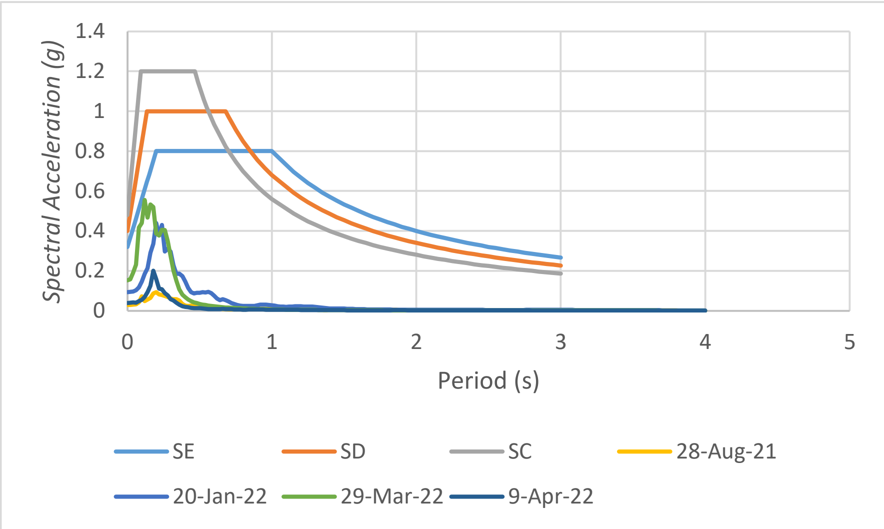

Figure 6. Comparison of response spectral accelerations of significant earthquakes with response spectra designs in SNI 1726:2019 at JGPI Station

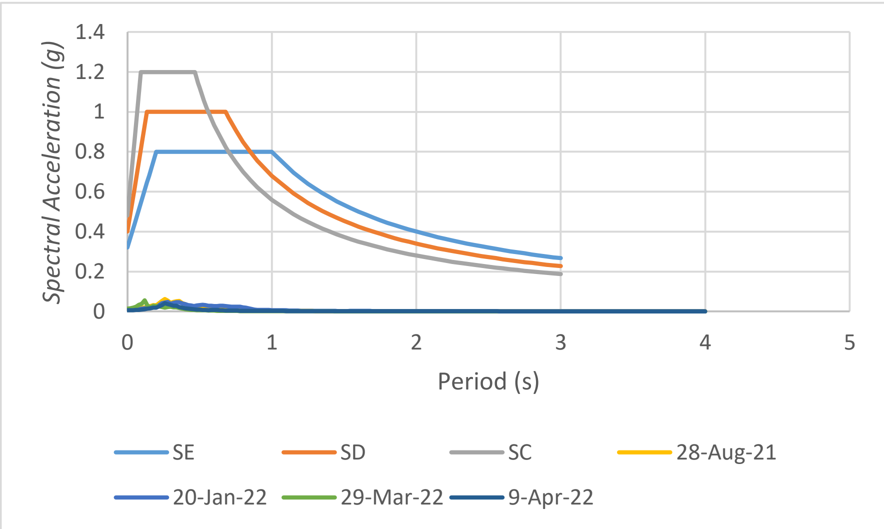

Figure 7. Comparison of response spectral acceleration significant earthquakes with response spectra designs in SNI 1726:2019 at JBPI Station

Response spectra designs contained in SNI 1726:2019 refer to FEMA P-1050-2015, the NEHRP Recommended Seismic Provisions for New Buildings and Other Structures. The response spectral acceleration parameters of the risk-targeted maximum considered earthquake (MCE_R) were mapped at short period (0.2 s) and long period (1 s). The PGA bedrock map is based on SNI 1726:2019 and developed based on a 2% probability of exceedance in 50 years. Generally, the spectral acceleration values of all earthquakes at both JBPI and JGPI Stations are relatively lower than those of response spectra designs in SNI 1726:2019, as seen in Figures 6 and 7.

4. Conclusions

The analysis results show a higher PGA value in JGPI Station than in JBPI Station. The PGA value in JGPI Station is consistent with its distance to the epicenter, whereas that in JBPI Station is not in direct proportion to distance. Site conditions, distance to the epicenter, magnitude, and other factors can affect the PGA value at each station. JBPI Station has a longer effective duration than JGPI Station due to the site conditions of JBPI Station which has relatively softer soils. Furthermore, response spectral acceleration values of all earthquakes at both JBPI and JGPI Stations are relatively lower than those of response spectra designs in SNI 1726:2019. This indicates that the earthquakes were felt but did not cause damage, as per the actual conditions.

Acknowledgment

The author would like to express the deepest appreciation to BMKG for the support and provision of earthquake data, enabling the successful completion of this study. The author is also extremely grateful to the anonymous reviewer for the inputs and suggestions to improve the quality of this manuscript.

References

[1] Charlton, T. R. *Tertiary Evolution of the Eastern Indonesia Collision Complex*. Journal of Asian Earth Sciences 18. 603-631, 2000.

[2] Hall, R. & Spakman W. *Subducted Slabs Beneath the Eastern Indonesia-Tonga Region: Insight from Tomography*. Earth and Planetary Science Letters 201, 321-336, 2002.

[3] Tregoning P. & Gorbatov A. *Evidence for active subduction at the New Guinea Trench*. Geophysical Research Letter 13, L13608, 2004.

[4] Visser W. A. & Hermes J. J. *Geological Results of the Exploration for Oil in Netherlands New Guinea: Carried Out by The Nederlandsche Nieuw Guinee Petroleum Maatschappij 1935-1960*. S'gravenhage, Staatsdrukkerij-En Uitgeverijberrif, 1962.

[5] Koswara A. *Peta Geologi Lembar Taritatu (Keerom), Irian Jaya, 1:250.000*. Pusat Penelitian dan Pengembangan Geologi, 1995.

[6] BPS Kota Jayapura. *Kota Jayapura Dalam Angka 2021*. Jayapura, 2021.

[7] Pawirodikromo W. *Seismologi Teknik dan Rekayasa Kegempaan*. Yogyakarta, 2012.

[8] BMKG. *Katalog Gempa Bumi Signifikan Dan Merusak*. Jakarta, 2019.

[9] Hiola, M. F. H., & Sunardi, B. *The Acceleration Response Spectrum And Effective Duration Of Lebak Earthquake January 23, 2018 In Jakarta Region. Spektra: Jurnal Fisika dan Aplikasinya*, *4*(1), 21-30, 2019.

[10] Herrmann, R. B., Malagnini, L., & Munafò, I. *Regional moment tensors of the 2009 L'Aquila earthquake sequence*. Bulletin of the Seismological Society of America, 101(3), 975-993, 2011.

[11] Mousavi-Bafrouei, S. H., & Mahani, A. B. *A comprehensive earthquake catalogue for the Iranian Plateau (400 BC to December 31, 2018)*, Journal of Seismology, 24(3), 709-724, 2020.

[12] Douglas, J. *Earthquake ground motion estimation using strong-motion records: a review of equations for the estimation of peak ground acceleration and response spectral ordinates*. Earth-Science Reviews 61 (1–2): 43–104, 2003.

[13] M. D. Trifunac & A. G. Brady. *A Study on the Duration of Strong Earthquake Ground-Motion*. Bulletin of the Seismological Society of America. Vol. 65, No. 3, pp. 581-626, 1975.

[14] Suwarna N. dan Noya Y. *Peta Geologi Lembar Jayapura (Peg. Cycloop) Irian Jaya*. Pusat Penelitian dan Pengembangan Geologi, 1995.

[15] Uang C.M, Bertero V.V. *Evaluation of Seismic Energy in Structures.* Earthquake Engineering and Structural Dynamics, Vol.l9, pp.77-90, 1990.

[16] Seismosoft. *SeismoSignal v5.1 – A computer program for signal processing of strong-motion data*. http://www.seismosoft.com, 2013.

[17] Kramer S L. 1996, *Geotechnical Earthquake Engineering*. Prentice Hall, New Jersey.

[18] Badan Standarisasi Nasional. *SNI 2847:2019 Persyaratan Beton Struktural untuk Bangunan Gedung*. Jakarta, 2019.

[19] PAZ, M. (1991*), Structural Dynamics: Theory and Computation*, 3rd Ed. Chapman & Hall, New York.